Hydrogeol J (2017) 25:1301–1317
DOI 10.1007/s10040-017-1548-6

PAPER

A coupled groundwater-flow-modelling and vulnerability-mapping methodology for karstic terrain management

Konstantina P. Kavouri[1] · **George P. Karatzas**[1] · **Valérie Plagnes**[2]

Received: 21 June 2016 / Accepted: 28 January 2017 / Published online: 24 February 2017

Abstract A coupled groundwater-flow-modelling and vulnerability-mapping methodology for the management of karst aquifers with spatial variability is developed. The methodology takes into consideration the duality of flow and recharge in karst and introduces a simple method to integrate the effect of temporal storage in the unsaturated zone. In order to investigate the applicability of the developed methodology, simulation results are validated against available field measurement data. The criteria maps from the PaPRIKa vulnerability-mapping method are used to document the groundwater flow model. The FEFLOW model is employed for the simulation of the saturated zone of Palaikastro-Chochlakies karst aquifer, in the island of Crete, Greece, for the hydrological years 2010–2012. The simulated water table reproduces typical karst characteristics, such as steep slopes and preferred drain axes, and is in good agreement with field observations. Selected calculated error indicators—Nash-Sutcliffe efficiency (NSE), root mean squared error (RMSE) and model efficiency (E′)—are within acceptable value ranges. Results indicate that different storage processes take place in different parts of the aquifer. The north-central part seems to be more sensitive to diffuse recharge, while the southern part is affected primarily by precipitation events. Sensitivity analysis is performed on the parameters of hydraulic conductivity and specific yield. The methodology is used to estimate the feasibility of artificial aquifer recharge (AAR) at the study area. Based on the developed methodology, guidelines were provided for the selection of the appropriate AAR scenario that has positive impact on the water table.

Keywords Karst · Aquifer modelling · Vulnerability mapping · Distributed recharge · Greece

✉ Konstantina P. Kavouri
dinakavouri@gmail.com

[1] School of Environmental Engineering, Technical University of Crete, Polytechneioupolis, 73100 Chania, Greece

[2] Sorbonne Universités, UPMC Univ Paris 06, CNRS, EPHE, UMR 7619 Metis, 4 place Jussieu, 75005 Paris, France

Introduction

The exploitation of water resources in many coastal carbonate aquifers relies on pumping wells. Also, in most cases, the natural output of coastal aquifers is submarine springs. Given the increased risk of overexploitation and seawater intrusion problems in these systems, coastal karst aquifers require specific management plans.

Numerical models have been widely employed in the field of groundwater resources management. In karst hydrogeology, lumped-parameter or black-box models are traditionally used to study the global response of the aquifer recharge. They are usually applied to karst systems with distinct measurable discharges such as one or more springs (Fleury et al. 2007; Le Moine et al.; 2008; Jukić and Denić-Jukić 2009; Charlier et al. 2012; Ladouche et al. 2014). The application of lumped parameter models requires long time series of input (precipitation) and output (spring discharge) variables. On the other hand, distributed parameter models are more applicable to management scenarios exhibiting spatial variability such as land use modifications and artificial recharge plans. Distributed parameter models take into consideration the spatial variations of the aquifer and allow the definition of variable conductivity fields, storage zones and boundary conditions. The main disadvantage of these models is that the limited knowledge regarding the geometry and spatial distribution of the hydraulic parameters of the aquifer may introduce a high degree of uncertainty to the results.

Over the past years numerous distributed parameter models have been developed and applied to karst aquifers following three principal modelling approaches: (1) equivalent porous continuum (EPC) (Teutsch and Sauter 1998; Scanlon et al. 2003; Dafny et al. 2010), (2) discrete fractures (DF) (Jeannin 2001), and (3) combined equivalent porous continuum with discrete fracture (EPC-DF) (Király 2002; Quinn et al. 2006; Liedl et al. 2003; Birk et al. 2006; de Rooij et al. 2013). According to Teutsch and Sauter (1991), the hybrid EPC-DF models are more adequate for large-scale modelling of karst; furthermore, the duality of infiltration and especially the role of epikarst has been addressed with the integration of epikarst models (Király 1998; Bauer et al. 2005; Fleury et al. 2007; Tritz et al. 2011) and the zonal distribution of recharge (Martínez-Santos and Andreu 2010; Chen and Goldscheider 2014; Hugman et al. 2012).

The present study aims to develop a methodology that allows for the management of karstic terrains with spatially heterogeneous infiltration conditions and for the implementation of artificial recharge plans. The proposed methodology combines elements from the vulnerability mapping method PaPRIKa (Drfliger and Plagnes 2009; Kavouri et al. 2011; Huneau et al. 2013) with groundwater flow models using the hybrid EPC-DF modelling approach. The model is developed using the finite element simulator FEFLOW, which allows for the integration of fractures at pre-specified areas of the model. Special attention is given to the realistic representation of the structural and functional characteristics of the karst and mainly to the spatial distribution of recharge.

The methodology is applied to the coastal karstic system of Palaikastro-Chochlakies, in the island of Crete, Greece. As part of a general framework for the sustainable management of the aquifer, a scenario for artificial aquifer recharge (AAR) is proposed and tested. The applied management scenario is designed on the basis of financial and technical feasibility. According to Daher et al. (2011), the ability for artificial recharging of a karst aquifer can be determined as a combination of intrinsic rechargeability and feasibility, in terms of the hydrogeological properties of the karst and of the techno-economic feasibility. Daher et al. (2011) proposed a multi-criteria methodology for the managed aquifer recharge of karst aquifers, the ARAK method. The criteria used in the aforementioned method are defined in accordance with intrinsic vulnerability mapping methods such as PaPRIKa. In the present study, the rechargeable zones of the aquifer are determined through both vulnerability mapping and modelling approaches, while the effect of AAR is also quantified.

Hydrogeology of the study area

The karst system of Palaikastro-Chochlakies is located in the carbonate terrain of eastern Crete and covers an area of 72 km^2 (Fig. 1). This karst system receives about 700 mm of rain annually. The recharge of the system is estimated to be 46% of mean annual precipitation, which corresponds to a mean volume of $93 \cdot 10^6$ m^3/year for the entire carbonate platform (IGME 2005). The aquifer body consists of a series of limestones and dolomites, approximately 600 m in thickness, that overlies the impermeable formation of the "Phyllite-Tyros bed" (Papanikolaou and Vassilakis 2010). The eastern boundary of the aquifer is the sea. Steeper contact surfaces are locally created as a result of the action of normal faults. Three principal fault directions have been reported: (1) N–S, (2) WSW–ENE and (3) E–W. The major N–S fault zone which transects the region has lowered the eastern part by tens of meters and has created a depressed zone approximately 1.2 km wide which was eventually covered by thick Miocene to Pleistocene sediments. Many karst features such as cavities, dolines and karstic gorges are present in the western part of the area. The geometry of the impermeable substratum of the aquifer appears to have an east inclination while steep slopes appear at the western part of the area (Fig. 2).

A submarine source of unknown discharge, located at the coastal area of Karoumpes, is the natural outlet of the Palaikastro-Chochlakies karst system. Also, minor outflows of fresh water are likely to emerge along the entire coastline. The intermittent spring of Flegas (elevation 220 m above sea level) is the only inland spring and is located inside the homonymous gorge at a distance of 5.3 km upstream from the coast. Flegas spring is the outlet of a perched paleokarstic system which drains a significant part of the upstream basin (Figs. 1 and 2). It yields approximately $3 \cdot 10^6$ m^3/year during the winter months and becomes dry approximately 2 months after the last rainfall (IGME 2005). The catchment area of the paleokarstic system of Flegas extends up to 18.5 km^2 west of the intermittent spring. The altitude difference between the paleokarstic system of Flegas and the underlying aquifer exceeds 150 m; therefore, the only possible hydraulic communication of the two systems is a limited leakage from the perched aquifer to the subjacent water table. A small loss of water to other aquifers is likely to take place at the northern border of the Palaikastro fault.

Of the 17 wells that have been recorded in the area, 13 pump water for irrigation purposes, 1 supplies water to the town of Palaikastro and 3 have no pumping infrastructure. According to drilling data, none of these wells intersects a karst conduit or part of the confined aquifer. The pumping rates vary from 35 to 120 m^3/h. Two unsuccessful drilling attempts have also been identified and mapped. A detailed description of the study area can be found in Kavouri and Karatzas (2016).

The proposed conceptual flow model for the coastal aquifer of Palaikastro-Chochlakies is presented in Figure 3 and it is based on the karst model presented by Mangin (1975). The unsaturated zone of the Palaikastro-Chochlakies karstic system consists of the epikarst, the soil and the zones of

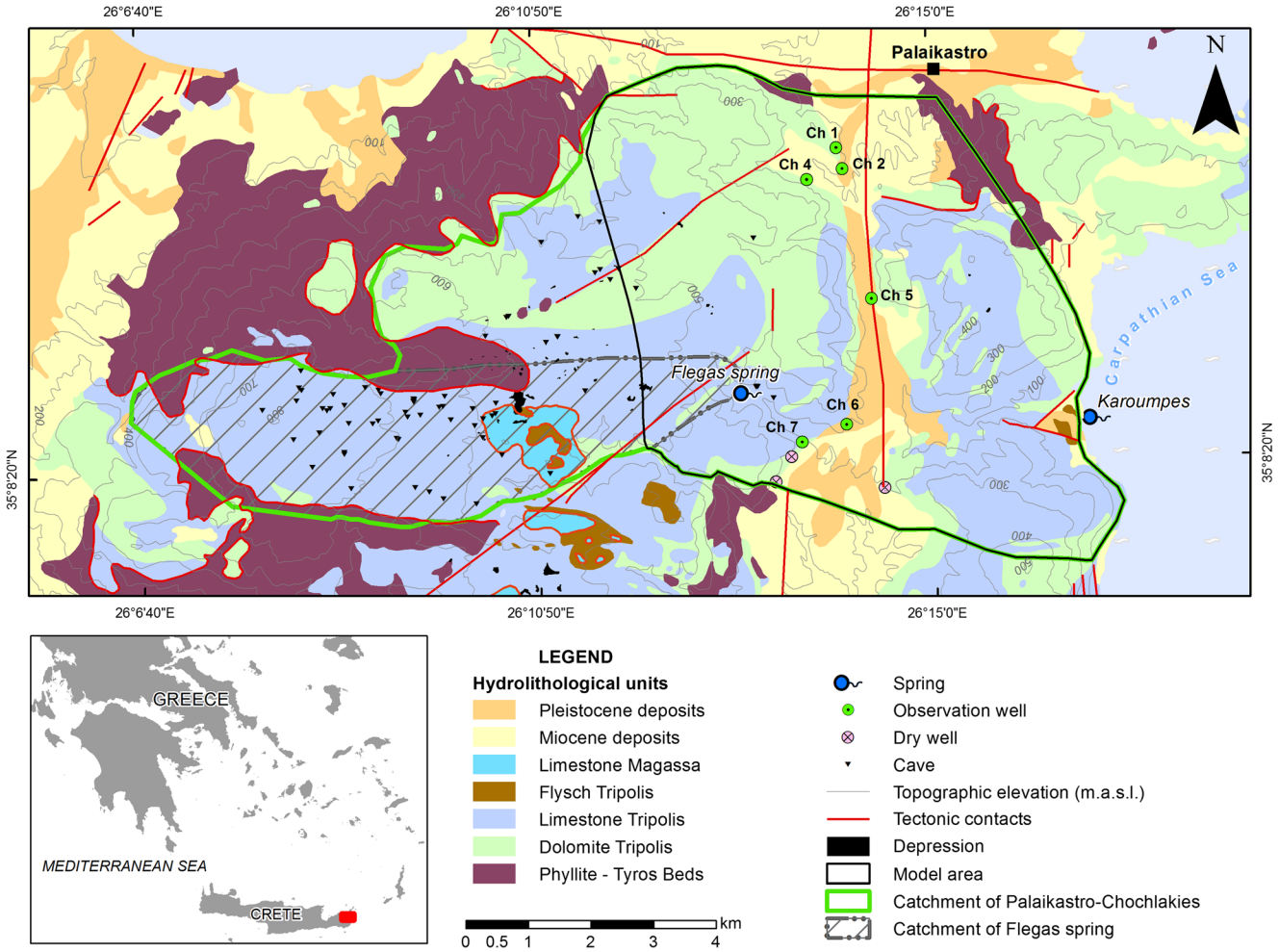

Fig. 1 A simplified hydrogeological map of the study area (modified after Kavouri and Karatzas 2016). The map is based on the geological cartography of IGME (Institute of Geology and Mineral Exploration of Greece 1959) at scale 1:50000, the work of Papanikolaou and Vassilakis (2010), and data from the speleological club of Crete and field observations

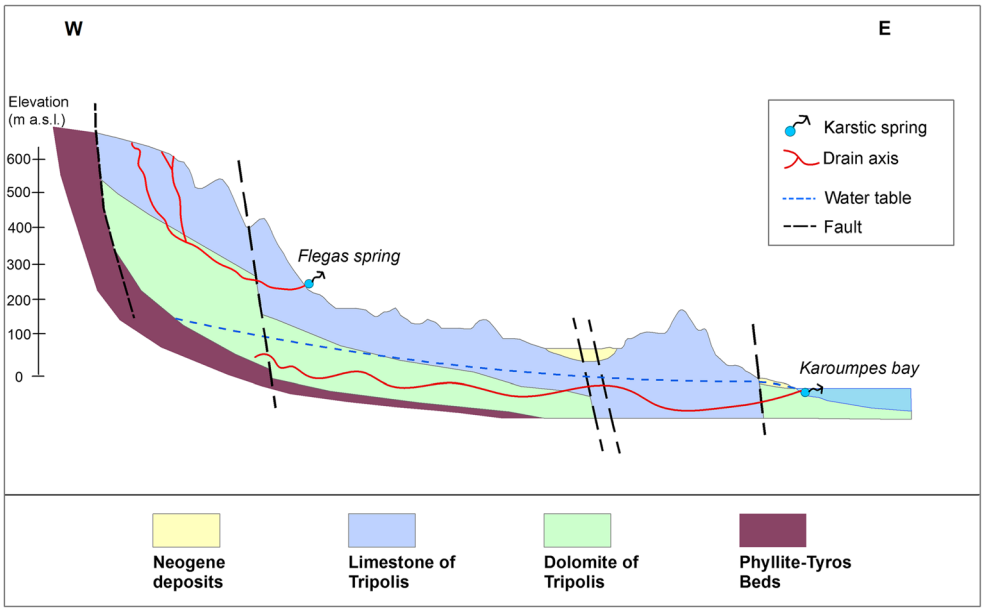

Fig. 2 Schematic profile of the coastal aquifer of Palaikastro-Chochlakies and the perched paleokarstic system of the *Flegas spring* (Kavouri and Karatzas 2016)

concentrated infiltration (i.e., sinkholes, fractures and dolines). Additionally, the unsaturated zone contains the perched paleokarst aquifer of Flegas and the homonymous spring. The saturated part of the aquifer contains the rock matrix, the drain axes and the annex-to-drain systems. The output of the system consists of the submerged spring and the diffuse coastal outflows at Karoumpes Bay, as well as the water pumped out of the system (Fig. 3). One principal drain axis can be considered to be the Karoumpes drain, which is located along the gorge of Flegas and ends at the submerged spring. Other major fractures are also present, such as the Palaikastro N–S fault which connects the northern part of the aquifer with the southern part. Infiltration through sinkholes, fractures and dolines follows vertical paths to the saturated zone, while rainwater entering the soil and epikarst is slowly directed to the annex-to-drain systems through both lateral and vertical percolation. This procedure is often characterized as diffuse infiltration (Fig. 3).

Methodology

The developed methodology is a combination of vulnerability mapping and groundwater flow modelling. Vulnerability mapping is a terrain-characterization tool that has been widely applied over the past years for the protection of groundwater resources in karstic areas. This vulnerability mapping also provides a basic spatial characterization of the system properties. In the present study, the criteria maps of the PaPRIKa vulnerability mapping method (Kavouri et al. 2011) are integrated in a distributed parameter model developed using the FEFLOW code.

FEFLOW (WASY) is a finite element code for groundwater modelling which allows for the integration of channel and pipe flow conditions in discrete features within the matrix (Diersch 2013). The finite element mesh facilitates the incorporation of heterogeneities in the model domain. Three different laws of fluid motion can be defined within the discrete features: Darcy's law for laminar flow, the Manning-Strickler law for open channel flow and the Hagen-Poiseuille law for pipe flow. For the simulation of free aquifers, FEFLOW uses the Best Adaptation to Stratigraphic Data (BASD) technique where the top slice of the model is determined by a free and movable surface that represents the water table (Diersch 2013).

Values were assigned to the hydraulic parameters of the model following a zonal distribution. The cartographic method PaPRIKa was used for the delimitation of the continuous zones. PaPRIKa is a multi-criteria geographic information system (GIS)-based mapping approach for the evaluation of the intrinsic vulnerability of karst. It combines four independently mapped criteria, protection (P), rock type (R), infiltration (I) and karstification (Ka). Five classes of vulnerability are distinguished for each criterion from very low to very high vulnerability (0–4). The protection and rock type criteria refer to the structure of the karstic terrain, while the Infiltration and the karstification criteria characterize the functional properties

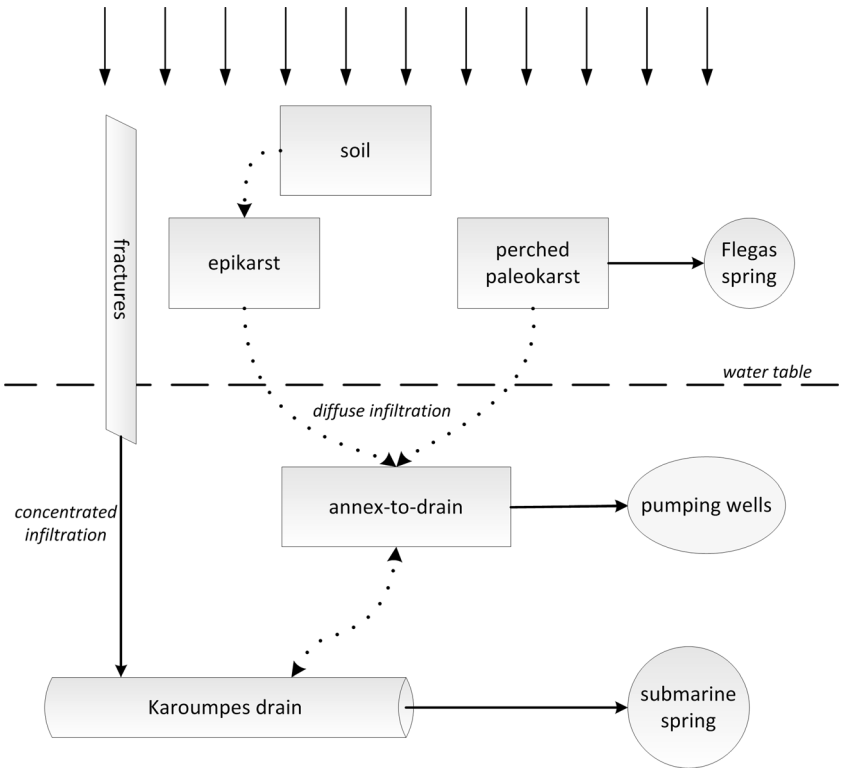

Fig. 3 Conceptual flow model for the karst aquifer of Palaikastro-Chochlakies

of the aquifer. The PaPRIKa method has been tested and evaluated at ten different karstic systems in France (Kavouri et al. 2011; Huneau et al. 2013). A detailed description of the method and of the definition of the criteria can be found in Dörfliger and Plagnes (2009).

Vulnerability mapping

First, the vulnerability mapping methodology was applied to the study area. Each criterion was mapped independently according to the method guidelines.

Rock type criterion: R map

The Palaikastro-Chochlakies karst aquifer is developed in the limestone and dolomite formations of the Tripolis unit. Both formations appear to have thick quasi-horizontal bedding. Regarding the lithology, the reservoir is classified as R_2 (moderate vulnerability), the areas that present networks of cavities and fault zones are mapped and classified as R_4 (very high vulnerability), while the areas around R_4 zones where the rock shows to have an important degree of fissuring, are classified as R_3 (high vulnerability).

Karstification criterion : Ka map

The *karstification criterion* (Ka) is based on speleological data and a geomorphological analysis while no tracer test data were available for the study area. Three active karstic conduits were mapped in the Palaikastro-Chochlakies catchment area by the Speleological Group of Crete. All three conduits are located in the upstream area of Flegas spring, and for this reason they have been assigned to the perched system of the intermittent spring; however, they are considered to have an important effect on the vulnerability of the subjacent aquifer, as they present strong vertical development. A buffer zone of 50 m around the mapped conduits is classified as Ka_4 (very high vulnerability).

Based on geomorphological and hydrogeological information such as drilling logs, there are strong indications for the existence of five more active conduits. These karstic conduits are plunged in the saturated zone of the Palaikastro-Chochlakies aquifer and constitute the principal flow paths of the aquifer. A buffer zone of 50 m around those conduits is classified as Ka_4 (very high vulnerability).

The areas around Ka_4 zones which have an important degree of fissuring are classified as Ka_3 (high vulnerability) and the rest of the area as Ka_2 (moderate vulnerability).

Infiltration criterion: I map

The *infiltration criterion* is based on slope analysis and karstic geomorphological features. For the assessment of the infiltration criterion, the catchment of each sinkhole is delineated on the topographic map (scale 1:5,000) and is classified as I_4 (very high vulnerability). Additionally, the karstic gorges are delineated and also classified as I_4 (very high vulnerability). Mapped depressions such as dolines are classified as I_3 (high vulnerability), except if they are integrated in the basin of an active sinkhole. Finally, the areas that do not include distinct exokarstic features are characterized based on the slope. The slopes of the studied zone are estimated with the use of GIS on the base of a 25-m digital elevation model.

Protection criterion: P map

The *protection criterion* is based on the cartography of the soil cover, the epikarst, the thickness and the structure of the unsaturated zone, and the catchment area of the Flegas perched aquifer. Temporal storage principally occurs in the thick Neogenic deposits of the northern part of the karstic system and especially in the conglomerate formations of the Miocene. The conglomerate formations of Miocene are classified as S_0 and the Holocene, Pleistocene and Pliocene deposits as S_1.

The unsaturated zone consists of thick bedded limestone and dolomite with sub-horizontal bedding (LUZ_2). The thickness of the unsaturated zone is greater than 50 m and the rock body presents significant fracturing (UZ_2). Epikarst represents a shallow layer of the carbonate column which is considerably more karstified and permeable than the rock located immediately below. In unconfined karst aquifers, where recharge mainly depends on direct infiltration, the presence of epikarst results in an almost constant recharge rate and controls the evapotranspiration process (Perrin et al. 2003; Bakalowicz 2005). The epikarstic layer of the carbonate rocks of the study area is well developed, having an average thickness of 0.2–0.4 m. It is generally classified as E_2 except for the areas near fractures and sinkholes where the epikarst is intersected by large vertical fractures and therefore is characterized as E_4. Finally, the entire catchment area of the perched aquifer of Flegas spring is classified as E_1.

The protection criterion is a combination of soil (S), unsaturated zone (UZ) and epikarst (E). In each point of the P map, the most protective value of all P sub-factors is retained in order to evaluate the effectiveness of the protective cover layers. The criteria maps resulting from the application of the PaPRIKa method to the study area are presented in Fig. 4.

Model development

Reservoir geometry, drain axes and fractures

Karst aquifer systems exhibit increased complexity regarding their structural and functional characteristics (Bakalowicz 2005; Goldscheider and Drew 2007; Ford and Williams 2007). The genesis and development of karst usually reflect major tectonic and climatic events that took place in the region. Additionally, the

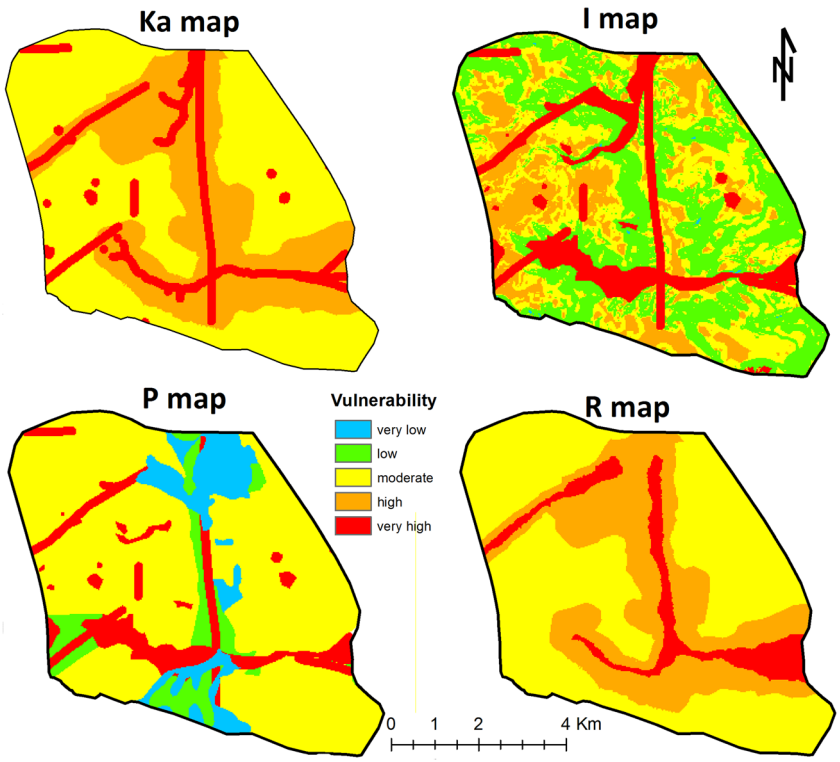

Fig. 4 The four criteria maps of the PaPRIKa method for the study area

geomorphologic evolution of the landscape can provide useful information on deeper karstic features. The study area has been subject to Neogene extensional stresses that resulted in the creation of normal faults. These faults have controlled the hydrodynamic evolution of the karst, by creating preferential flow paths. Consequently, the presence of ravines and dry valleys indicates the approximate location of drain axes.

A three-dimensional (3D) flow model was developed for the saturated zone of the karst aquifer (46 km^2; Fig. 5). The base-model consists of five layers, each defined by one upper and one lower slice. The bottom slice of the model represents the impermeable substrate of the model domain and has fixed geometry, while the top slice represents the water table and is defined as a free and movable surface. Fractures and drains are represented by 2D discrete features of 0.2–0.7 m thickness and open channel flow conditions. At the coastal zone, the drain of Karoumpes is assumed to be confined and is represented by a 1D discrete feature of 1.2 m thickness and pipe flow conditions.

The simulation period of the groundwater model is 2 years specifically for the time period 2010 to 2012. The time step is set to automatic step control—forward Euler/backward Euler (FE/BE) time integration scheme—and the initial time step is set to 0.001 days. The calibration is based on field measurements of water-table fluctuations realized at six observation wells (Ch1, Ch2, Ch4, Ch5, Ch6 and Ch7) during wet and dry periods of 2010–2012.

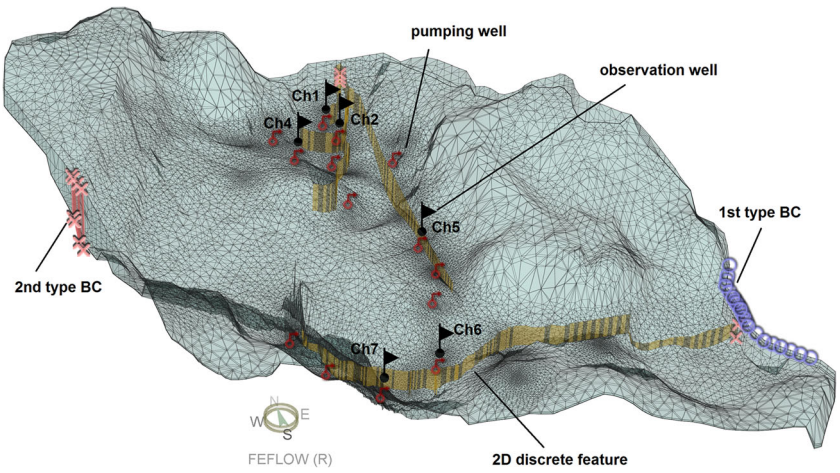

Fig. 5 Locations and types of boundaries conditions (*BC*) on the 3D flow model of the Palaikastro-Chochlakies aquifer

Initial heads and boundary conditions

The initial heads introduced to the model reproduce the water table of October 2010 based on ten field measurements. The measured values of water elevation were first interpolated by using the Kriging method and then used as initial heads for a steady-state simulation. The heads calculated from the steady-state simulation were next fed to the transient state model. A constant head of 0 m was assigned along the sea border (first type boundary condition). Second type, no-flux boundary conditions were assigned at the northern, northeastern and southwestern borders of the domain where the impermeable layer outcrops. A lateral influx second type boundary condition was assigned around the faulted zones of the northwestern border. The southwestern border of the model is assumed to receive zero lateral influx because of the perched paleokarstic system of the Flegas spring. The submerged spring at the Karoumpes Bay and the northern border of the Palaikastro fault were represented by second type boundary conditions, the values of which were calibrated. The boundary conditions applied on the developed model are presented in Fig. 5.

Hydraulic conductivity and specific yield

The delimitation of hydraulic conductivity fields is in accordance with the *rock type criterion* of the PaPRIKa method (Fig. 6). Since lithologically the aquifer is practically homogeneous, differentiation relies on the degree of fracturing. Higher values of conductivity are assigned to the areas corresponding to R_4 zones. An intermediate conductivity zone is maintained for R_3 and the lowest values of hydraulic conductivity are assigned to R_2 zones. The values of hydraulic conductivity for horizontal axes (Kxx and Kyy) are of the order of 10^{-5} and 10^{-7} m/s according to the pumping tests performed in the intermediate zone, while for the vertical axis (Kzz) hydraulic conductivity values are equal to 1/10 of the horizontal at the corresponding node. It is noted that the present values characterize only the fractured matrix and not the karst aquifer in total. The bottom slice of the model represents the impermeable substrate and it is constrained. Conduit flow is simulated by 2D discrete features as explained in section 'Reservoir geometry, drain axes and fractures'. The delimitation applied to hydraulic conductivity applies to specific yield as well. The sensitivity of the model to changes in hydraulic conductivity and specific yield is studied in section 'Sensitivity analysis'.

Definition of stress periods

In order to take into consideration the dual character of infiltration in karstic systems, the hydrological year was divided into four stress periods, based on local hydrological and meteorological conditions and pumping schedules (Fig. 7): SP1, from October to January, SP2 from February to April, SP3 from May to June, and SP4 from July to September. SP1 and SP2 represent the wet period of the hydrological year. SP1 includes the first 4 months of the hydrological year whose precipitation events are of prime importance for the replenishment of the reservoir according to Kessler (1965). During these 4 months, approximately 65% of the annual precipitation falls within the catchment area. SP2 consists of rainy months with the greatest chance of flash rainfall events. SP3 stands for the recession period of the Flegas spring and represents the minimum time required for the diffuse infiltration to reach the saturated zone. It should be mentioned that the length of this period is probably underestimated for the karst aquifer of Palaikastro-Chochlakies, because the perched aquifer of Flegas has a much smaller catchment area and is

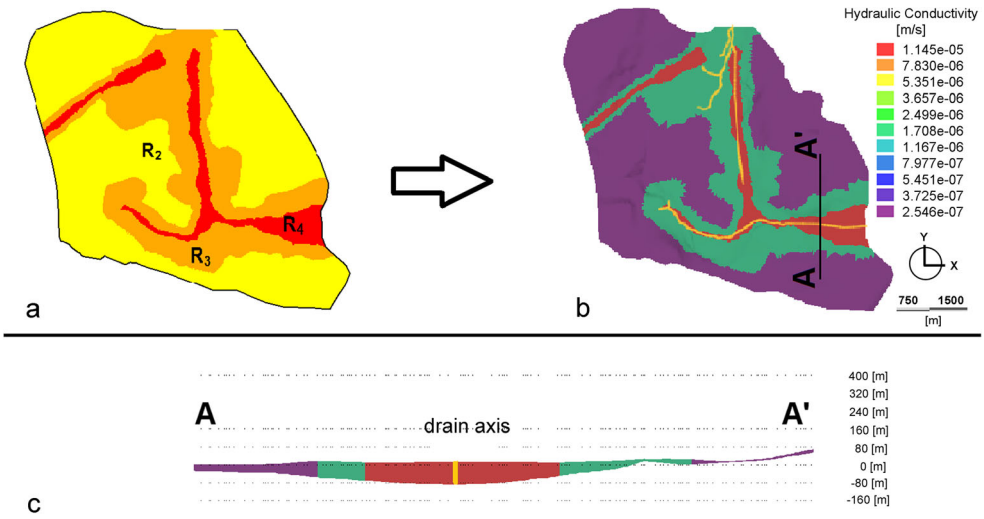

Fig. 6 **a** R map of PaPRIKa vulnerability method, and **b** the delimitation of hydraulic conductivity zones based on part **a**; **c** cross section showing the vertical distribution of hydraulic conductivity field

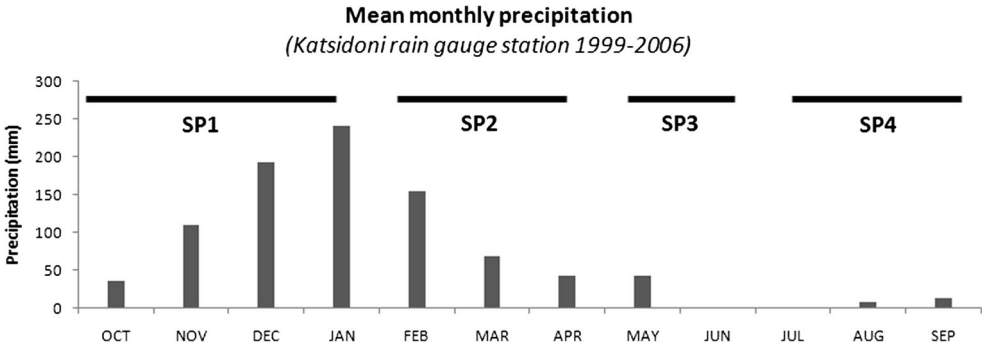

Fig. 7 Mean monthly precipitation at Katsidoni rain gauge station and partitioning into stress periods [data source: Prefecture of Crete]

considerably more karstified than the subjacent aquifer of Palaikastro-Chochlakies. Finally, the recharge is practically zero during SP4. Pumping for irrigation purposes takes place during SP3 and SP4, while the pumping well for water supply is constantly active.

This classification is helpful when considering diffuse infiltration conditions, whereas for concentrated infiltration it is unnecessary. When water percolates fast through the unsaturated zone, the transit time is negligible and defining stress periods becomes redundant. In this case, data may be employed as a function of the available precipitation recordings.

Effective infiltration

The calculation of effective infiltration takes into account the fact that prolonged water storage near the surface may result in high evapotranspiration (ET), especially during the summer months. In contrast, the effect of ET in zones of fast vertical infiltration is negligible. The zonal characterization of the carbonate terrain with respect to effective infiltration is based on the Protection and Infiltration criteria of the PaPRIKa method, as they are described in Dörfliger and Plagnes (2009). Consequently, the effective infiltration map includes five classes (Fig. 8a):

- Class F, including fault zones, sinkholes, dolines and their catchments (I_3 and I_4)
- Class S, for permeable soils (P_1)
- Class M, for marl deposits (P_0)
- Class K, for nude limestone and epikarst (P_2)
- Class P, for the perched aquifer of the Flegas spring (P_1)

The effective infiltration percentage proposed for each class is presented in Table 1. The values for class K (nude limestone, epikarst) and class P (perched aquifer) are in accordance with the empiric coefficients of infiltration for karstic terrains proposed by Kessler (1965) and tested by Soulios (1984) in three karstic regions of Greece. The Kessler coefficients have been adjusted to the applied stress periods as presented in Table 2. In the Kessler method, the coefficient for the month of March is 113%, as the method was developed in areas with snow during the winter months. In this study, the coefficient for March has been reduced to 90%, since there is no snowfall in the region.

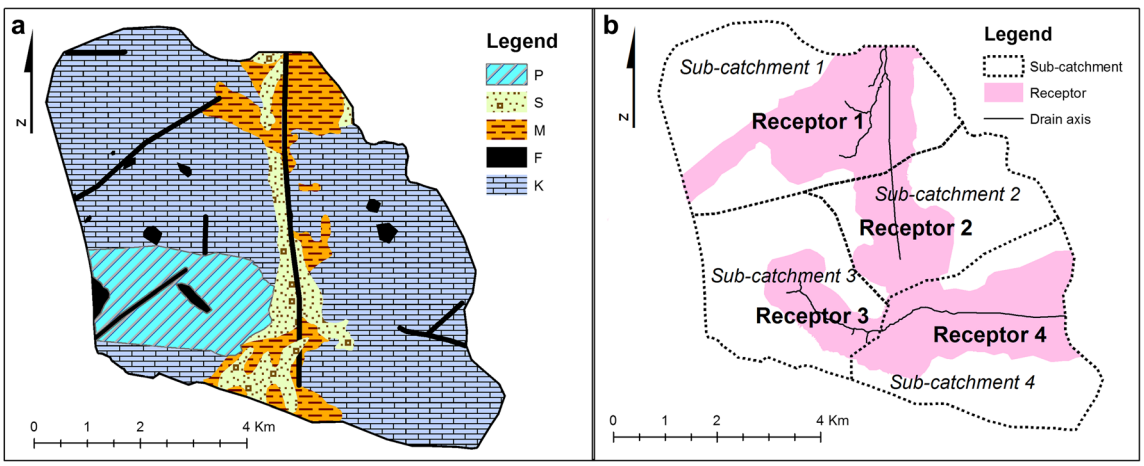

Fig. 8 **a** Classes of effective infiltration, and **b** Spatial distribution of recharge receptors, sub-catchments and discrete features

Table 1 Effective infiltration percentage for the five classes of the Infiltration map

Class	Description	Effective infiltration (%)			
		October–January	February–April	May–June	July–September
F	Fault zone, sinkhole, doline	90	90	60	60
S	Covered with soil	25	25	10	10
M	covered with marls	10	10	1	1
K	Nude limestone – epikarst	35	80	40	17
P	Perched aquifer	35	80	40	0

The vegetation is limited to the areas of soil development and consists of olive trees. For permeable soils, the infiltration coefficient is set to 25% for SP1 and SP2 and 10% for SP3 and SP4, according to estimated values for the Neogene deposits presented in a report of the Institute of Geology and Mineral Exploration of Greece (IGME) for the hydrogeological conditions in eastern Crete (IGME 2005). For the relatively impermeable marl deposits, the infiltration coefficient is set to 10% for SP1 and SP2 and 1% for SP3 and SP4.

Two different approaches are applied depending on the defined infiltration class. The first approach includes class F, where fast infiltration occurs, and ET is practically zero. In this class, the notation *i*, which represents the month, is used for the infiltration volume calculation. The second approach accommodates for classes S, M, K and P, where diffuse infiltration takes place, and ET is important. In these classes, the notation *j* is used which represents the stress period.

The infiltrated volume (VI_{ij}), for all classes, is given by equation:

$$VI_{i,j} = P_{i,j} \times AI \times EI_{i,j} \quad (1)$$

whereterms in the following are:

$VI_{i,j}$ the infiltrated volume [L^3]
$P_{i,j}$ the precipitation events that fall over the area for each period i, j [L]
AI the extent of the implicated infiltration zone [L^2]
$EI_{i,j}$ the effective infiltration percentage
i 1–12, representing month (for fast infiltration)
j 1–4, representing stress period (for diffuse infiltration)

Recharge

In this study, recharge is defined as the volume of water that reaches predefined areas of the water table divided by time. In karst aquifers, recharge is a spatially and temporally distributed variable which depends on the thickness and the structure of the infiltration zone. According to the present conceptual model, infiltration follows either fast and vertical or slower and more complex pathways through the unsaturated zone until it reaches the water table. Furthermore, in developed unconfined karst, where organized drain structure is anticipated, infiltrated water is more likely to reach the water table at the locations of the drains and of the annex-to-drain-systems.

Table 2 Adjusted values of Kessler coefficient per stress period and estimated infiltration for class K

Month	Stress period	Mean monthly rainfall (mm)	Kessler coefficient	Mean monthly infiltration (mm)	Adjusted Kessler coefficient for class K per stress period	Mean infiltration for class K (48% of total karstic terrain)
Oct	SP1	50.90	12.8	6.50	35	126.02
Nov		95.47	22.5	21.48		
Dec		110.63	49.7	54.98		
Jan		135.60	43.4	58.85		
Feb	SP2	82.09	77.5	63.62	80	139.84
Mar		63.05	113.0 | 90	71.24 | 56.74		
Apr		22.33	60.0	13.94		
May	SP3	13.90	44.6	6.19	40	6.21
Jun		1.92	33.9	0.65		
Jul	SP4	0	20.7	0	17	0.15
Aug		0.12	17.6	0.02		
Sep		5.82	14.6	0.84		
Total	–	581.83	–	283.13	–	272.22
%	–	100%	–	51% | 48%	–	47%

The delimitation of the recharge receptor is based on the definition of the karstification criterion of the PaPRIKa method and corresponds to the areas included in classes Ka_3 and Ka_4, zones of high and very high vulnerability due to karstification. Finally, the recharge receptor is divided into four regions corresponding to the contributions of four sub-catchment areas defined by geomorphologic criteria (Fig. 8b). The influence of recharge receptors in the efficiency of the model is presented in Kavouri and Karatzas (2016).

The infiltrated volumes originating from zone F are imported monthly to the aquifer, whereas the infiltrated volumes originating from zones S, M, K and P are calculated separately for each sub-catchment and they are introduced to the model as a mean rate for each stress period to corresponding receptors.

The perched paleokarstic system of the Flegas spring constitutes an independent aquifer system, which is assumed to extend over the entire catchment area of the intermittent spring. The discharge of the spring is recorded daily by IGME. The contribution of the perched system to the subjacent aquifer is estimated from the difference between input and output water volumes of the annual budget and corresponds to approximately 7% of the total infiltrated volume. Recharge originating from the paleokarstic system is attributed to receptor 3 with a constant rate over SP1, SP2 and SP3. Recharge is imported with the in/outflow on the top/bottom module of FEFLOW as a time dependent variable (Fig. 9).

Calibration

Hydraulic head calibration was realized in transient state conditions for hydrological years 2010–2012. The hydrological years 2010–2011 and 2011–2012 are representative of the mean annual precipitation for the studied area. Measurements were taken twice a year, during the wet and dry period, from the six observation wells shown in Fig. 1. The parameters of the model are presented in Table 3.

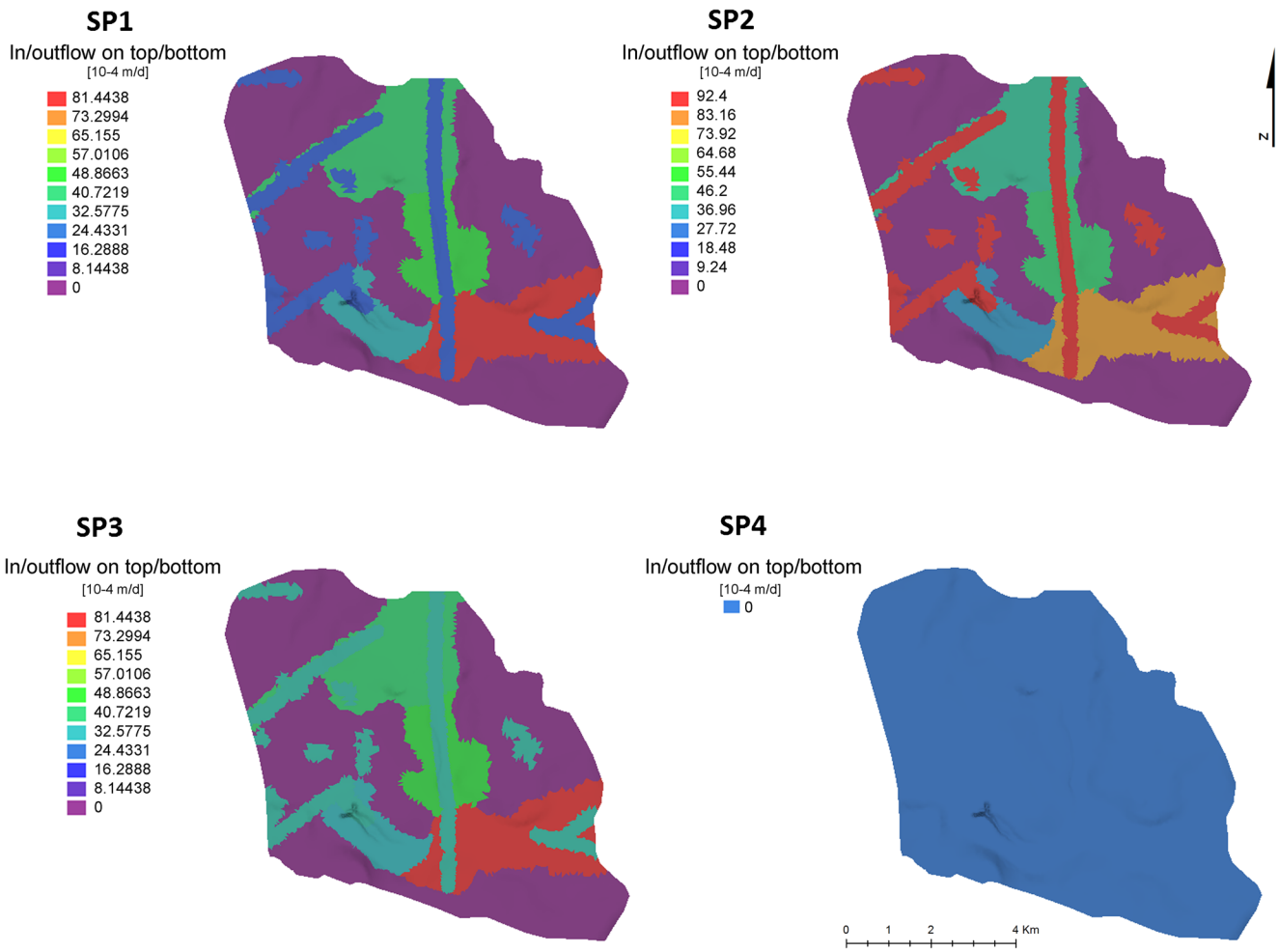

Fig. 9 Distribution of recharge for each stress period (hydrological year 2011–2012)

Table 3 Model parameters

Parameter	Distribution	Value
Kxx, Kyy, Kzz	Zonal (R criterion)	Estimated from pumping test data/calibrated
Specific yield	Zonal (R criterion)	Estimated from pumping test data/calibrated
Initial heads	Interpolated	Measured October 2010
BC 1st type	Nodal	$h = 0$
BC 2nd type	Nodal	Estimated/calibrated
Recharge (in flow on top)	Zonal (Ka criterion and major faults)	Estimated by recharge model
Wells	Nodal	Pumping schedule
Drains	Discrete feature	Calibrated
Reservoir geometry	Interpolated	Geology, borehole data

Kxx, *Kyy*, *Kzz* refer to hydraulic conductivity, *BC* boundary condition, *h* hydraulic head

For the model calibration, the Nash-Sutcliffe efficiency (NSE), the root mean squared error (RMSE) and model efficiency (E′) indicators were used (Moriasi et al 2007):

$$\mathrm{NSE} = 1 - \frac{\sum_{i=1}^{N}(O_i - P_i)^2}{\sum_{i=1}^{N}\left(O_i - \overline{O}\right)^2} \quad (2)$$

$$\mathrm{RMSE} = \sqrt{\frac{\sum_{i=1}^{N}(O_i - P_i)^2}{N}} \quad (3)$$

$$\mathrm{E}' = 1 - \frac{\sum_{i=1}^{N}|O_i - P_i|}{\sum_{i=1}^{N}\left|O_i - \overline{O}\right|} \quad (4)$$

where P_i is the predicted hydraulic head value at observation point i and O_i the observed value at the same point. $\bar{O}$ is the mean observed hydraulic head over N the observation points.

The NSE coefficient describes model efficiency and its values range between $-\infty$ and 1 (perfect fit). Efficiency values lower than zero indicate that the mean of the observed data would have been a better predictor than the model. The NSE coefficient is commonly used in hydrological modelling. RMSE is a measure of the differences between predicted and observed values of hydraulic head and is expressed in length units. RMSE is a simple error indicator that is easily interpreted. E′ indicates the goodness of fit between observed and forecasted stream flow and its values range between 0 and 1 (perfect fit).

Results

Modelling results

The observed and simulated water tables are in good agreement despite the large range of the values of hydraulic heads (Fig. 10). The NSE coefficient was calculated equal to 0.96, E′ equal to 0.79 and RMSE equal to 2.23 m. The model is capable of reproducing the system operation under transient state conditions for both wet and dry periods.

The water budget of the model is positive and equals $7 \cdot 10^6$ m^3/year for 2012. During SP1 and SP2, the water table rises as a result of significant recharge. The water table regresses during SP3 and SP4 when irrigation pumping takes place. The rate of water level decline presents noticeable differences between the north-central and the southern part of the aquifer. In the north-central part of the aquifer, 45% of the total water level drawdown occurs by the end of SP3, while in the southern part, drawdown has reached 82% of the total annual by the end of the same period (Fig. 11). This indicates different storage processes in different parts of the aquifer. Specifically, the north-central part seems to be more influenced by diffuse recharge processes than the southern part. The southern part is more affected by concentrated recharge, and for this it is better correlated to precipitation events.

The northern and central parts of the system receive approximately 6.8×10^6 m^3 of water per year, 27% of which is extracted from the aquifer in order to cover the demand for water supply and irrigation. The water table is smooth and hydraulic head fluctuations between wet and dry periods do not exceed 4 m.

In the southern part of the aquifer, the water table presents very steep slopes as a result of the major drain axis of Karoumpes. Water-table fluctuations may reach 8 m according to measurements performed at observation well Ch7 and according to simulation results. Recharge is rapidly directed to the karstic drain and then to the sea, keeping at low levels the storage capacity of this part of the aquifer. Additionally, the southern part of the aquifer is controlled by the constant head boundary condition along the coastal zone. The losses calculated at the coastal zone are approximately $3.2 \cdot 10^6$ m^3, which corresponds to 52% of the total annual recharge at the sub-

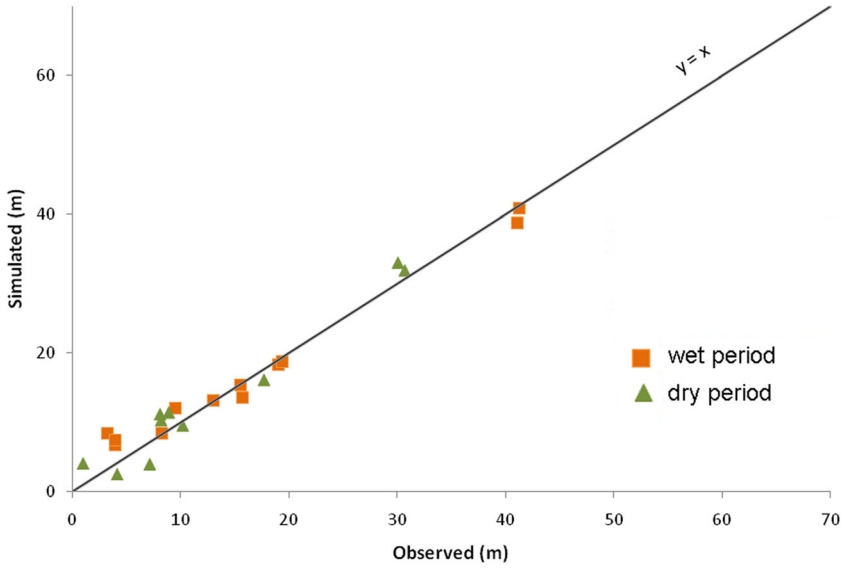

Fig. 10 Simulated versus observed values for the hydraulic head in the observation wells for the period 2010–2012

catchments 3 and 4. About half of these losses take place during SP3 and SP4, when the aquifer replenishment by recharge is minimized.

In general, the water table presents steep slopes around the drain axes and highly fractured areas due to the difference in hydraulic characteristics between the high- and low-conductivity zones and due to the unconstrained flow within fractures (Fig. 12).

Sensitivity analysis

Sensitivity analysis tests are performed for the hydraulic conductivity and specific yield model parameters. The values of hydraulic conductivity and specific yield for the performed sensitivity analysis tests are changed by ±10, ±25, ±50 and ±150%. Error indicators NSE, RMSE and E′ are used as quantification criteria. The results of the sensitivity analysis are presented in Table 4.

Results do not vary significantly and the sensitivity of both parameters is rather low. The model exhibits greater sensitivity to changes in hydraulic conductivity than to changes in specific yield. Specifically, greater sensitivity is more apparent for the 150% variation of hydraulic conductivity which represents non-realistic values of the parameter. It is observed that RMSE reflects better the sensitivity of the examined parameters. This indicator is also easier to employ when comparative analysis is required as it is expressed in length units.

Future management scenarios

In eastern Crete, there is practically no natural replenishment of the groundwater resources during the summer months. By contrast, the demand for potable and irrigation water increases significantly during the same period. Water demand in the study area has increased over the last years due to the rapid

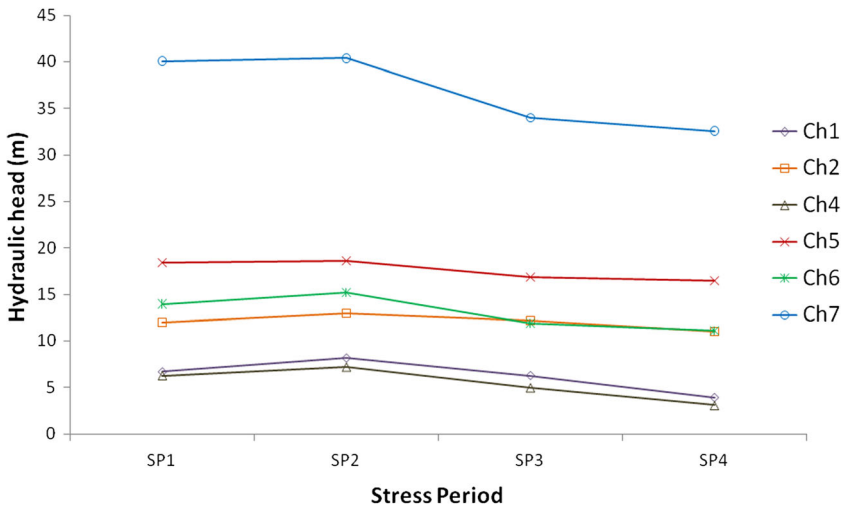

Fig. 11 Annual fluctuations in hydraulic head (simulated values for the period 2011–2012)

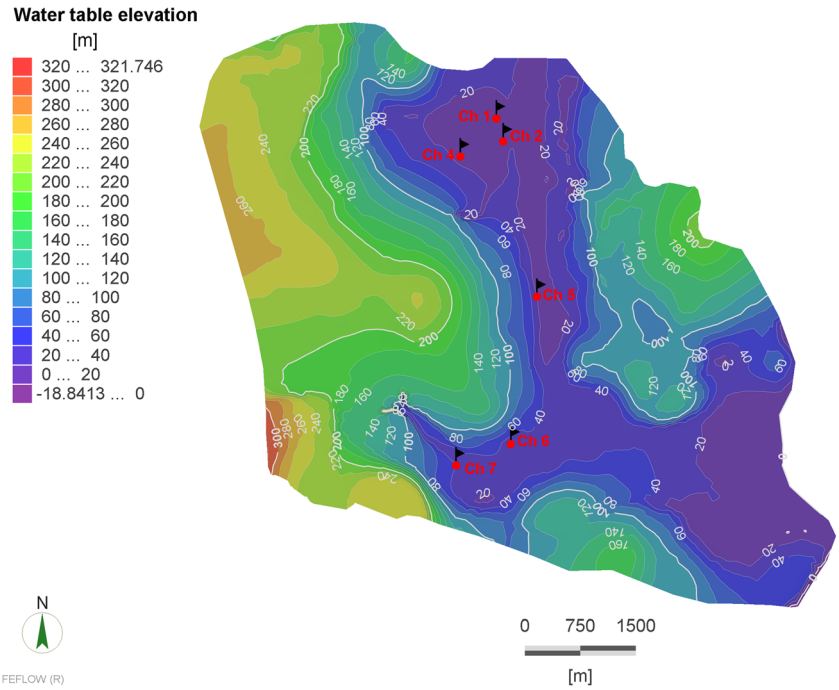

Fig. 12 Simulated water table for the dry period of 2012

development in tourism and in the energy industry. In order to cover the increased water demand, the local community wishes to manage the water discharge from the intermittent spring of Flegas which remains unexploited to date.

A management scenario of artificial aquifer recharge (AAR) is examined in this study, according to which 70% of the discharge of the Flegas spring is imported to the Palaikastro-Chochlakies karst aquifer through injection wells. The proposed scenario is theoretical and its scope is to acquire a first estimation on the aquifer's ability to positively respond in artificial recharge.

Artificial aquifer recharge

Artificial recharge is a way to store water in the subsurface in times of water surplus in order to meet water demands in times of shortage (Andelman et al. 1994). It is a commonly applied method in arid and semi-arid regions. There exist different AAR techniques including the use of injection wells, galleries and spreading basins (Bouwer 2002). Xanke et al. (2016) developed a 2D model to simulate water-table fluctuations of managed storm water recharge through an infiltration reservoir and pumping in a karst aquifer in Jordan; however, AAR is not always feasible or cost-effective in karstic terrains (Daher et al. 2011). A successful AAR design for karst should avoid water injection in the principal drain axes of the system, as these areas generally provide short-term water storage. On the other hand, injection wells in the matrix have the risk of being insufficient due to the low hydraulic conductivity of the fissured rock. Generally, AAR projects in karstic terrains are based on site-specific methodologies.

Application of AAR on the Palaikastro-Chochlakies karst aquifer

The intermittent spring of Flegas is an important source of good quality fresh water in the area. It discharges annually approximately 9–10 million of cubic meters of water and it

Table 4 Sensitivity to hydraulic conductivity and specific yield. Results for parameter value changes by ±10%, ±25%, ±50%, ±150%

Parameter	Error indicator	Simulation error	+10%	−10%	+25%	−25%	+50%	−50%	+150%	−150%
Hydraulic conductivity	NSE	0.960	0.953	0.96	0.944	0.957	0.922	0.949	0.786	0.873
	RMSE	2.226	2.402	2.231	2.621	2.304	3.099	2.52	5.160	3.964
	E′	0.790	0.785	0.780	0.765	0.768	0.706	0.747	0.523	0.628
Specific yield	NSE	0.960	0.959	0.959	0.957	0.954	0.955	0.941	0.939	0.878
	RMSE	2.226	2.239	2.243	2.307	2.392	2.357	2.704	2.748	3.125
	E′	0.790	0.782	0.793	0.775	0.781	0.766	0.756	0.743	0.645

goes dry during the summer months. This water flows towards the sea, unexploited. The use of the Flegas spring discharge as a recharge source would not require pretreatment and clogging effects would be unlikely to occur because of the low content of suspended particles in spring water. In the scenario under consideration, 70% of the spring discharge is used for the replenishment of the Palaikastro-Chochlakies karst aquifer and the rest 30% flows to the sea. For the simulation period 2011–2012, the mean injected water volume is estimated to be 11,000 m^3 for SP1, 25,000 m^3 for SP2, and 3,000 m^3 for SP3. No water injection is applied for SP4.

The selection of the appropriate locations for the implementation of AAR takes into consideration the specific characteristics of the site. According to the proposed conceptual model for the Palaikastro-Chochlakies karst aquifer, four interconnected recharge receptors are distinguished in the saturated zone of the aquifer, alimented each by a corresponding sub-catchment (Fig. 8b). Receptor 1 is located in the northern part of the site and includes one water supply well (Ch4). Due to its distance from the Flegas spring and out of concern for the water supply well, Receptor 1 is not preferable for the implementation of ARR from the discharge of the Flegas spring. Receptors 3 and 4, located in the southern part of the site, are connected to the sea through the Karoumpes drain. Water storage in these two receptors is more likely to be short-term or unsuccessful and, therefore, the implementation of AAR in these areas is not recommended. Finally, receptor 2 is located in the central part of the site in a zone protected from sea intrusion. Additionally, it connects receptors 1 and 3, facilitating water exchange along the entire system and, finally, it is situated near the recharge source. For these reasons the proposed AAR scenario targets receptor 2. According to this scenario supplementary recharge is imported to the receptor 2 through 10 injection wells.

The artificial recharge source consists of 70% of the Flegas spring discharge. The recession period of the Flegas spring, which lasts approximately two months, is represented by stress period SP3. During this period there is almost no precipitation, while spring discharge is still significant. By injecting the discharge from the spring into the aquifer, a prolonged recharge of two months is already achieved.

The calculation of effective infiltration depends on the applied AAR technique. For example, the use of spreading basins would result in higher evapotranspiration. Daher et al. (2011) proposed the use of injection sub-horizontal wells or galleries in order to achieve greater spreading of the injected water. The choice of the appropriate method requires detailed field investigations and is beyond the scope of the present study. For the proposed AAR scenario, recharge is imported to the entire area of receptor 2. This area covers approximately 3.5 km^2 and is situated in the plains of the study area. Within this area, 10 theoretical injection wells, located in slice 3 of the model (Fig. 13c-d), were considered. The injection rate is set to 100 m^3/h; thus, five injection wells are enabled during SP1 (Inj1–Inj5), 10 during SP2 (Inj1–Inj10) and 1 during SP3 (Inj1).

The resulting hydraulic heads for the wet and dry periods are presented in Fig. 13c–d. The effect of AAR is mainly observed in the results for the dry period. This is due to the prolongation of the recharge period from SP1-SP2 to SP1-SP3. Except for the central area of the aquifer where AAR is implemented, the water table is also elevated in the northern part which corresponds to receptor 1. Finally, there is no significant variation in the southern part of the aquifer, because water flow is mainly controlled by constant heads at the coastal zone and fast drainage through karstic drains. The influence on the water table after the implementation of AAR is clearer in the arithmetic values of simulated hydraulic heads, which are presented in Table 5.

Methodology limitations

The aim of the developed model is to enhance the understanding of the aquifer. A good understanding of the way the aquifer functions is a precondition for the implementation of drastic management plans such as AAR. The proposed methodology provides guidelines for the selection of the most appropriate areas for the implementation of the AAR plan with respect to aquifer particularities. The effect of AAR can be estimated at a time scale equal to the length of the applied stress period; therefore, the accuracy of the model output is relative to the length of the stress periods, which are defined with respect to the infiltration rates. In karstic terrains, infiltration rates are a function of the degree of karstification of the aquifer and usually vary in space. Spatial limitations on the applicability of the methodology are related to the accuracy of the input data. Geophysical surveys, sedimentary characterization or dye tracer tests are techniques that could provide more detailed information on the feasibility of the AAR plan, and provide best accuracy in local scale.

Conclusions

In the present study, a new methodology for the management of karst aquifers is proposed and applied to the coastal karstic system of Palaikastro-Chochlakies in eastern Crete, Greece. The proposed methodology combines groundwater flow modelling with vulnerability mapping, in order to achieve a realistic representation of the karst operation. The conversion of the criteria maps of the PaPRIKa method into input parameters for the model can provide a simplified framework for karst modelling. The methodology is also in accordance with the widely accepted conceptual flow model for karst introduced by Mangin in 1975.

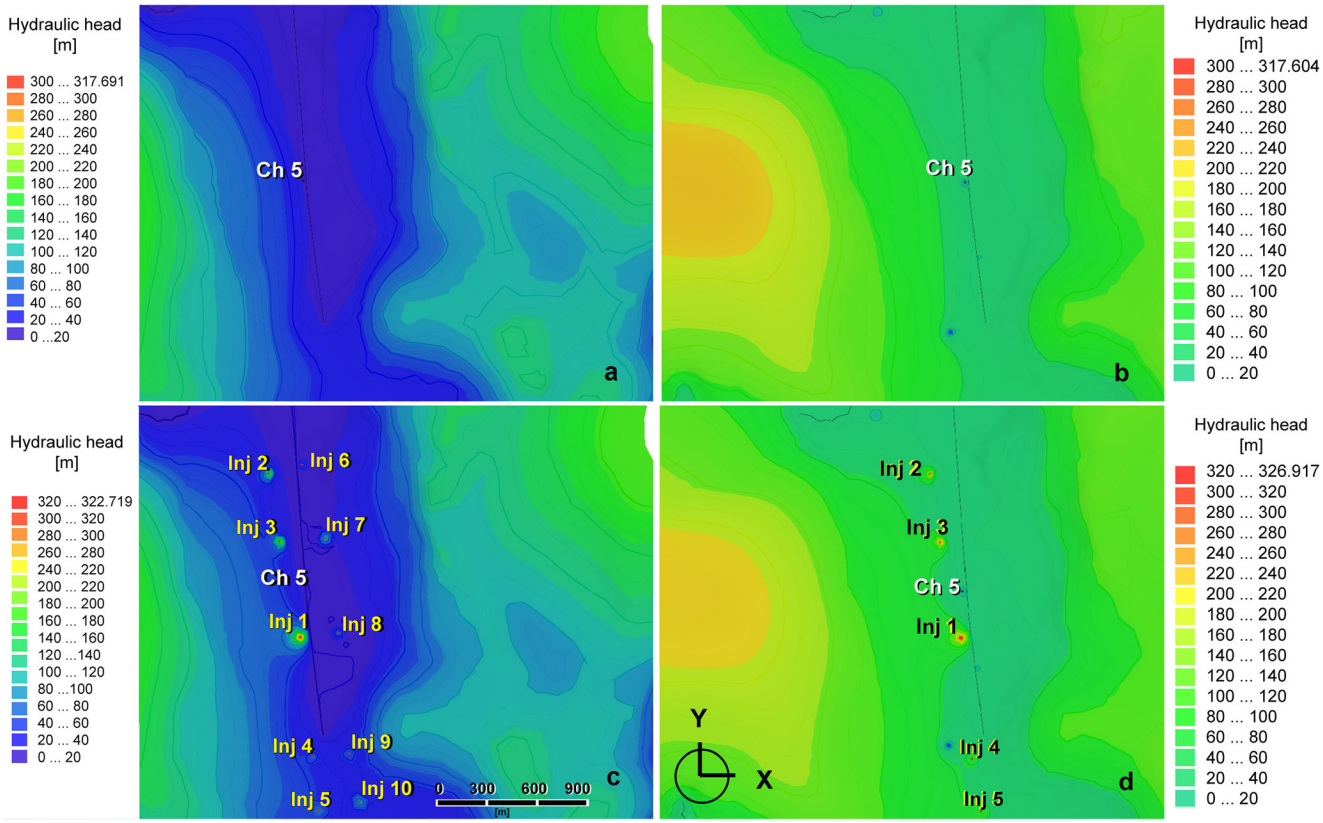

Fig. 13 A close-up view of the central area. Simulated hydraulic heads for: **a** the wet period of 2012, **b** the dry period of 2012 **c** the wet period of 2012, after implementing AAR and **d** the dry period of 2012, after implementing AAR

The duality of flow in the saturated zone was addressed with the integration of 1D and 2D discrete features within the matrix. The duality of the recharge process was approached with the introduction of customized stress periods, spatially variable infiltration zones and the definition of recharge receptors. The simulated hydraulic heads are in good agreement with field observations and the calculated error indicators are within acceptable ranges. Finally, the results of a sensitivity analysis indicate higher sensitivity of the model to changes in hydraulic conductivity than in specific yield.

Simulation results for the hydraulic heads indicate different storage processes in different parts of the aquifer. The north-central part seems more sensitive to diffuse recharge during SP3 (May to June) than the southern part, which is controlled by constant head boundary conditions and rapid flow within the major drain axis of Karoumpes.

Table 5 Simulated hydraulic heads *h* (m) at the observation wells before and after implementing AAR

Observation wells and scenarios		SP1		SP2		SP3		SP4	
		h	Δ*h*	*h*	Δ*h*	*h*	Δ*h*	*h*	Δ*h*
Ch1	Natural conditions	6.7	+5.5	8.2	+5.8	6.3	+6.6	3.9	+7.2
	AAR	12.2999		14.0		12.9		11.1	
Ch2	Natural conditions	12.0	+4.7	13.0	+4.7	12.2	+5.1	11.0	+5.1
	AAR	16.7		17.7		17.3		16.1	
Ch4	Natural conditions	6.3	+8.1	7.2	+8.4	5.0	+9.4	3.1	+10.5
	AAR	14.4		15.6		14.4		13.6	
Ch5	Natural conditions	18.42	+3.1	18.6	+3.5	16.9	+3.6	16.5	+3.5
	AAR	21.5		22.1		20.5		20.0	
Ch6	Natural conditions	14.0	+9.3	15.2	+9.3	11.9	+9.0	11.1	+9.4
	AAR	23.3		24.5		20.9		20.5	
Ch7	Natural conditions	40.1	+0.1	40.4	−0.1	34.0	+0.2	32.6	+0.5
	AAR	40.2		40.3		34.2		33.1	

The application of AAR to the studied aquifer appears very promising. The simulated AAR scenario had a positive effect on the water table especially during the dry period. The feasibility of the implementation for such a scenario is high, both because of the favorable intrinsic characteristics of the aquifer and of the easily accessible source of ample fresh water.

Limitations of the methodology are also to be considered. The limited knowledge of the aquifer geometric characteristics introduces an elevated degree of uncertainty. It should be stressed that the model adequacy also depends on the definition of recharge rates for diffuse infiltration zones. The estimated recharge rates determine stress periods. It is suggested that the length of each stress period be used as the minimum time interval for which the model prediction is valid. The presentation of the model results should also be in respect to the applied stress periods.

The developed methodology can be applied to catchment-scale modelling and to hydrogeological problems that require long-term analysis. The methodology could provide a useful tool for the management of groundwater resources with pumping wells, the design and implementation of AAR plans, and for land use planning, in general. The overall scope of the proposed methodology is to provide a standardized framework for addressing practical difficulties in karst modelling, such as the limited knowledge of the aquifer geometry and the scarcity of data.

Acknowledgements This work is part of doctoral research conducted at the Technical University of Crete, Greece, in collaboration with Dr Valérie Plagnes from the Pierre and Marie Curie University, France. The contribution of Mr G. Koinakis, geologist at IGME, branch of Crete, is greatly appreciated. Software licensing for the FEFLOW model was kindly provided by DHI.

References

Andelman J, Bauwer H, Charbeneau R, Christman R, Crook J, Fan A, Yates M (1994) Groundwater recharge using waters of impaired quality. Natl. Academy Press, Washington, DC

Bakalowicz M (2005) Karst groundwater: a challenge for new resources. Hydrogeol J 13(1):148–160

Bauer S, Liedl R, Sauter M (2005) Modeling the influence of epikarst evolution on karst aquifer genesis: a time-variant recharge boundary condition for joint karst-epikarst development. Water Resour Res 41, W09416. doi:10.1029/2004WR003321

Birk S, Liedl R, Sauter M (2006) Karst spring responses examined by process-based modeling. Ground Water 44(6):832–836

Bouwer H (2002) Artificial recharge of groundwater: hydrogeology and engineering. Hydrogeol J 10(1):121–142

Charlier JB, Bertrand C, Mudry J (2012) Conceptual hydrogeological model of flow and transport of dissolved organic carbon in a small Jura karst system. J Hydrol 460:52–64

Chen Z, Goldscheider N (2014) Modeling spatially and temporally varied hydraulic behavior of a folded karst system with dominant conduit drainage at catchment scale, Hochifen-Gottesacker. Alps J Hydrol 514:41–52

Dafny E, Burg A, Gvirtzman H (2010) Effects of Karst and geological structure on groundwater flow: the case of Yarqon-Taninim Aquifer, Israel. J Hydrol 389:260–275

Daher W, Pistre S, Kneppers A, Bakalowicz M, Najem W (2011) Karst and artificial recharge: theoretical and practical problems—a preliminary approach to artificial recharge assessment. J Hydrol 408:189–202

de Rooij R, Perrochet P, Graham W (2013) From rainfall to spring discharge: coupling conduit flow, subsurface matrix flow and surface flow in karst systems using a discrete-continuum model. Adv Water Resour 61:29–41

Diersch HJG (2013) FEFLOW finite element subsurface flow and transport simulation system. User's manual/reference manual/white papers, Release 6.2. WASY, Berlin

Dorfliger N, Plagnes V (2009) Cartographie de la vulnérabilité des aquifères karstiques guide méthodologique de la méthode PaPRIKa [Mapping the vulnerability of karst aquifers: guidelines of the method PaPRIKa]. Report BRGM RP-57527-FR, BRGM, Orleans, France, 100 pp

Fleury P, Plagnes V, Bakalowicz M (2007) Modelling of the functioning of karst aquifers with a reservoir model: application to Fontaine de Vaucluse (South of France). J Hydrol 345(1):38–49

Ford D, Williams PW (2007) Karst hydrogeology and geomorphology. Wiley, Chichester, UK

Goldscheider N, Drew DP (2007) Methods in karst hydrogeology. Taylor and Francis, London

Hugman R, Stigter T, Monteiro JP, Nunes L (2012) Influence of aquifer properties and the spatial and temporal distribution of recharge and abstraction on sustainable yields in semi-arid regions. Hydrol Process 26:2791–280. doi:10.1002/hyp.8353

Huneau F, Jaunat J, Kavouri K, Plagnes V, Rey F, Dörfliger N (2013) Intrinsic vulnerability mapping for small mountains karst aquifers, implementation of the new PaPRIKa method to Western Pyrenees (France). Eng Geol 161:81–93

Institute of Geology and Mineral Exploration of Greece (1959) Geological map of Greece. Map Sheet Ziros, scale 1:50.000. IGME, Athens

Institute of Geology and Mineral Exploration of Greece (2005) Hydrogeological study of the Prefecture of Lassithi. Report IGME, IGME, Athens, 243 pp

Jeannin PY (2001) Modeling flow in phreatic and epiphreatic karst conduits in the Holloch Cave (Muotatal, Switzerland). Water Resour Res 37:191–200

Jukić D, Denić-Jukić V (2009) Groundwater balance estimation in karst by using a conceptual rainfall–runoff model. J Hydrol 373(3–4): 302–315

Kavouri K, Karatzas GP (2016) Integrating diffuse and concentrated recharge in karst models. Water Resour Manag. doi:10.1007/s11269-016-1528-y

Kavouri K, Plagnes V, Tremoulet J, Dörfliger N, Rejiba F, Marchet P (2011) PaPRIKa: a method for estimating karst resource and source vulnerability: application to the Ouysse karst system (southwest France). Hydrogeol J 19:339–353. doi:10.1007/s10040-010-0688-8

Kessler H (1965) Water balance investigation in the karstic region of Hungary. Proc. Assoc. Int. Hydrogeol. Sci. (A.I.H.S.), UNESCO Symp. on Hydrology of Fractured Rocks, Dubrovnik, Croatia, July 1965, pp 90–105

Király L (1998) Modelling karst aquifers by the combined discrete channel and continuum approach. Bull Centre Hydrogéol 1998(16):77–98

Király L (2002) Karstification and groundwater flow. In: Proc. of the conference Evolution of Karst: Prekarst to Cessation. Zalozba ZRC, Postojna-Ljubljana, Slowenia, pp 155–190

Ladouche B, Marechal JC, Dorfliger N (2014) Semi-distributed lumped model of a karst system under active management. J Hydrol 509: 215–230

Le Moine N, Andréassian V, Mathevet T (2008) Confronting surface-and groundwater balances on the La Rochefoucauld-Touvre karstic

system (Charente, France). Water Resour Res 44(3), W03403. doi: 10.1029/2007WR005984

Liedl R, Sauter M, Hückinghaus D, Clemens T, Teutsch G (2003) Simulation of the development of karst aquifers using a coupled continuum pipe flow model. Water Resour Res 39(3):1057. doi: 10.1029/2001WR001206

Mangin A (1975) Contribution à l'étude hydrodynamique des aquifères karstiques [Contribution to the hydrodynamic study of karstic aquifers]. PhD Thesis, Université de Dijon, France, 422 pp

Martínez-Santos P, Andreu JM (2010) Lumped and distributed approaches to model natural recharge in semiarid karst aquifers. J Hydrol 388(3–4):389–398

Moriasi DN, Arnold JG, Van Liew MW, Bingner RL, Harmel RD, Veith TL (2007) Model evaluation guidelines for systematic quantification of accuracy in watershed simulations. Trans ASABE 50(3):885–900

Papanikolaou D, Vassilakis E (2010) Thrust faults and extensional detachment faults in Cretan tectono-stratigraphy: implications for Middle Miocene extension. Tectonophysics 488:233–247

Perrin J, Jeannin PY, Zwahlen F (2003) Epikarst storage in a karst aquifer: a conceptual model based on isotopic data—Milandre test site, Switzerland. J Hydrol 279:106–124

Quinn J, Tomasko D, Kuiper A (2006) Modeling complex flow in karst aquifer. Sediment Geol 184:343–351

Scanlon BR, Mace RE, Barrett ME, Smith B (2003) Can we simulate regional groundwater flow in a karst system using equivalent porous media models? Case study, Barton Springs Edwards aquifer, USA. J Hydrol 276(1):137–158

Soulios G (1984) Infiltration efficace dans le karst hellénique [Effective infiltration into Greek karst]. J Hydrol 75:343–356

Teutsch G, Sauter M (1991) Groundwater modeling in karst terranes: scale effects, data acquisition and field validation. Proc. 3rd Conf. on Hydrogeology, Ecology, Monitoring and Management of Ground Water in Karst Terranes. Nashville, TN, December 1991, pp 17–38

Teutsch G, Sauter M (1998) Distributed parameter modelling approaches in karst-hydrological investigations. Bull Hydrogeol 16:99–109

Tritz S, Guinot V, Joudre H (2011) Modelling the behavior of a karst system catchment using non-liner hysteretic conceptual model. J Hydrol 397:250–262

Xanke J, Jourde H, Liesch T, Goldscheider N (2016) Numerical long-term assessment of managed aquifer recharge from a reservoir into a karst aquifer in Jordan. J Hydrol 540:603–614